DIAGNOSE OF BIOMOLECULES USING RAMAN INTERACTIONS OF THE LIGHT

DIAGNOSTICUL BIOMOLECULELOR FOLOSIND INTERACȚIUNI RAMAN ALE LUMINII

CZU: 543.424.2 **https://doi.org/10.59295/spd2024n.113**

Marina TURCAN,
ORCID: 0000-0002-4514-8813
e-mail: marina.turcan@ifa.usm.md
Institute of Applied Physics, Moldova State University

Summary. *It is particularly important by now to apply the light in processing and development of modern diagnostic. Here with, two basic aspects of the interaction of light with the substance are discussed: the nonlinear one of light interaction with the environment, and the cooperative aspect of interaction of photons with matter (atoms or biomolecules). One should mention the use of metamaterials for tissue decontamination where the specific form of contact surface plays an important role. Another goal of the present work is the study and use of the cooperative effects of bacteria and viruses located in the evanescent field of biomaterials during Raman interaction of light in ultraviolet region. A model is proposed based upon existing experiments which takes into account the local symmetry of biomolecules. New models emerging from the non-linear interaction of the atomic (molecular) subsystem and the electromagnetic field of cavity could be elaborated. The photons statistic is proposed for the diagnosis of the new collective processes.*

Keywords: modern diagnostic, atoms or biomolecules, metamaterials, ultraviolet region, non-linear interaction.

INTRODUCTION

In this paper we describe the Raman spectroscopy, the types of these, application of this effect in physical, biomedical and chemical field. Therefore, Raman spectroscopy is a powerful technique which can distinguish between healthy and unhealthy cells and cancerous and nonmalignant cells.

It has been successfully utilized to determine qualitatively and quantitatively the molecular compositions of solid, liquid, and gases samples. The nonlinear theory of the excitation of vibration modes of bio-molecule of viruses and bacteria is proposed, taking into consideration the bimodal coherent states in coherent Raman excitation of biomolecules.

According to N. Blombergen [1], the coherent nonlinear Raman spectroscopy observed in 1963 will yield many new results in the next half-century. The third order susceptibility is composed of parts that depend on the presence of a vibrational mode and parts that are purely electronic in nature, which are known as the resonant and

non-resonant contributions, respectively. In 1974, Begley et al [2] summarized the most important advantages of vibrational spectroscopy based on nonlinear coherent anti-Stokes generation mechanism, which is five orders of magnitude stronger relative to spontaneous offers signals that are over Raman scattering. In several circumstances, this nonlinear technique avoids interference with a one-photon excited fluorescence background that often plagues conventional Raman measurements. This technique with the name coherent anti-Stokes Raman spectroscopy (CARS), and the authors of Ref. [2] reported the method as an attractive tool for rapid vibrational spectroscopy. For dappling the Ultrashort pulsed (USP) lasers in Coherent Raman Scattering (CRS) or CARS in the decontamination procedure of viruses 75 and bacteria in many cases it is necessary to know and use the proposed models, not only in the relative dimensions of viruses and bacterias but their symmetry too [4]. For destroying the dangerous virus structures dappling the CRS and CARS in many cases, it is necessary to know not only virus dimensions but the symmetry, topology and structure elements of viruses and bacteria. Most natural viruses depend upon the existence of spherical capsids: protective shells of various sizes composed of protein subunits. So far, general evolutionary pressures shaping capsid design have remained elusive, even though an understanding of such properties may help in rationally impeding the virus life cycle and designing efficient nano-assemblies.

Raman microscopy is a promising technology for visualizing the distribution of molecules in cells. A challenge for live-cell imaging using Raman microscopy has been long imaging times owing to the weak Raman signal. The protocol for constructing and using a Raman microscope equipped with both a slit-scanning excitation and detection system and a laser steering and nanoparticle-tracking system was done already by authors from [5]. Furthermore, its utility can be expanded to small-molecule imaging by using tiny Raman-active tags such as alkyne. For example, DNANA synthesis in a cell can be visualized by detecting a deoxyuridine derivative with an alkyne moiety. The authors describe the optics, hardware and software to construct the Raman microscope, and discuss the conditions and parameters involved in live-cell imaging [5]. Below we analyze a part of types of the technics Raman which are more applicable in different domains in specially in medicine and physics. For this reason, we explain how to interact photons in Raman process.

When a photon of light interacts with a molecule, it can induce a short-lived transition to a virtual energy state (Fig. 1). This temporary increase in energy means that the molecule is in a higher or virtual energy state. The molecule can relax back to the initial ground state in a single step by releasing the same amount of energy as that of the incoming photon—this processis known as Rayleigh (or elastic) scattering. As the energy of a photon is proportional to its frequency, and since no energy is transferred to the molecule, Rayleigh scattered light does not yield any information about the molecules under investigation.

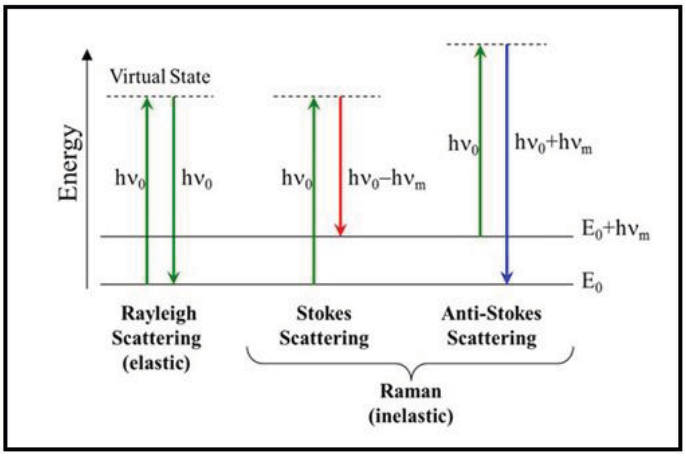


Figure 1. Rayleigh scattering diagram (elastic) and non-elastic Raman scattering [6].

However, relaxation can also occur in an inelastic manner — when a molecule releases a different quantity of energy to that of the incident photon. This phenomenon is known as Raman scattering; due to nuclear motion, energy can be transferred to or from the incident photon. There are two types of Raman scattering—Stokes and anti-Stokes scattering. In the case of Stokes scattering, energy can be transferred to the molecule from the incident photon via nuclear motion within the molecule, resulting in a scattered photon of reduced energy and hence reduced frequency. Conversely, in a smaller proportion of molecules energy is transferred to the photon as, due to the distribution of thermal energy, these molecules are initially in a higher energy state. This is anti-Stokes scattering [7]. In biomedical research, Stokes scattering is most commonly observed and the signal is inherently weak.

If we get into the CARS case and compare with another effect stimulated Raman scattering (SRS) we have advantage at the detection. Nonlinear coherent Raman effects such as coherent anti-Stokes Raman scattering (CARS) and stimulated Raman scattering (SRS) enhance the weak Raman signal by means of nonlinear excitation. When the energy difference between two laser beams exciting a sample matches a molecular vibration, resonance occurs that enhances the intensity of light generated at the anti-Stokes frequency (CARS signal) or induces a change in the excitation beam intensity (SRS signal). The CARS or SRS signal is usually several orders of magnitude stronger than spontaneous Raman. This has enabled video-rate imaging to be achieved [5]. Another advantage is that these techniques allow detection of the Raman band even from strong fluorescent samples, because the detection of CARS or SRS is not affected by fluorescence. The CARS signal is emitted at a higher frequency, which does not overlap with one-photon fluorescence, whereas SRS is detected at the excitation field frequency by radio-frequency lock-in detection. A drawback of these techniques is the complexity of the setup, as the two lasers are needed to combine both temporally and spatially. And

thus far, these techniques have been demonstrated only for strong Raman bands from chemical species with high concentrations. For example, CH2-stretching vibrations, which are typically found in high concentrations in cells as lipids, produce strong CARS and SRS signals.

In SERS, a metallic nanostructure interacts with incident photons, which generates an enhanced electric field in the vicinity of the metal surface. When a target molecule exists near the surface of a metallic nanostructure, Raman scattering is markedly enhanced. SERS has been widely used in biomedical applications because of its high-sensitivity detection and molecular selectivity [8]. Recently, we published results from an experiment in which a gold nanoparticle was introduced into a cell as a dynamic SERS probe analyzing the biochemical composition of its immediate surroundings during its travel inside the cell. We constructed a laser-tracking Raman microscope that follows one particular particle of interest and continuously observes the SERS from the particle. The simultaneous tracking and SERS measurement capability of our Raman microscope allowed us to probe cellular transport pathways, for example, endocytosis and organelle transport.

The paper is organized as follows. A short description and characterization of the methods in introduction, experimental and theoretical approach. The setup and theoretical mechanism of the action of UV-radiation for decontamination are presented in second section.

1. The Raman spectroscopy description

Raman spectroscopy can distinguish between healthy and unhealthy cells and cancerous and nonmalignant cells [1]. Thus, Raman spectroscopy is a powerful technique for label-free identification and characterization with potential for translation to biomedical and clinical applications. The Raman spectrum provides a measure of the vibrational mode density of molecules that can be translated to biochemical content. In the spontaneous Raman process, (see Figure 2(a)), a narrow band laser illuminates the sample and a portion of the incident photons is scattered by interactions with molecular vibrations, resulting in a shift to higher (anti-Stokes) or lower frequency (Stokes) photons. In the CARS process, two laser beams with different wavelengths (816 nm—pump/probe beams and 1064 nm—Stokes beam) coherently excite a particular vibrational mode, see Figure 2(b). For CARS, the laser source consists of two time-locked pulse trains of different wavelengths (pump + Stokes) such that the difference in photon energy corresponds to the vibrational mode to be imaged. The anti-Stokes photon is detected indicating the strength of the signal at a given vibrational mode. The UV radiation is largely absorbed by matter, and the purification of water or other biological liquid needs small volumes. In order to exclude this question, i.e., decontamination of small volumes, an efficient method was proposed, based on evanescent field technique created around silica metamaterials. When UV light is propagated through an optical fiber, significant quantity of radiation is spread outside of the fiber as an evanescent field that interacts with surrounding medium. Optical techniques play an important role for localization of

nanometric and submicronic particles. Such methods, based on optical metamaterials (e.g., photonic crystals, optical fibers or cavities) where the penetration of evanescent field in the contaminated zone is primordial, can be used as an efficient decontamination procedure for viruses and microorganisms [13]. In the following, will be provide a theoretical description of the interaction of UV radiation with viruses, explaining the physical mechanism.

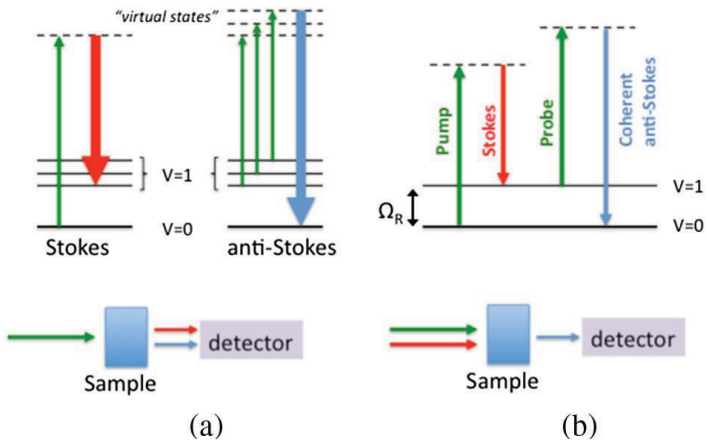


Figure 2. Principle of Raman scattering mechanisms of (a) spontaneous Raman and (b) narrowband CARS shown by Jablonski diagram (energy level diagram). Arrows represent photons (longer length denotes higher photon energy), V is the vibrational level, Ω_R is the resonant vibrational frequency of a given vibrational mode [9].

2. Description of the methods of decontamination

Cooperative conversion of the photons from Stokes in anti-Stokes modes stimulated by a stream of atom flying through the micro-cavity two standing waves were give in our paper [7]. The Hamiltonian that describes the interaction of the atoms with Stokes and anti-Stokes modes of the cavity electromagnetic field (EMF) can be represented through the atomic and field operators was done. In order to describe the collective processes, we introduced in Hamiltonian the collective operators for bimodal field, which are described by SU(2) symmetry. This reduction to SU(2) symmetry helps us to solve exactly the superradiant conversion between the Stokes and anti-Stokes photon using the conservation law of Bloch vector [7]. Still here on the Bloch sphere was presented the Laser working point. During the pulse, propagation in the fibre wave mode the new pulse is generated due to the scattering conversion of the photons in anti-Stokes (or Stokes) mode becomes possible in the process of relaxation (excitation) of the atoms trapped in the evanescent zone of the fibre. In Fig. 3 the red part of the pulse is the Stokes component and the blue part corresponds to the anti-Stokes one.

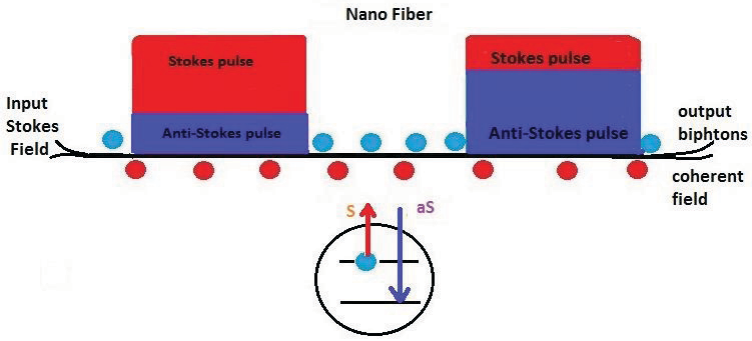


Figure 3. Propagation of Stokes pulse through nanofiber and its conversion in anti-Stokes pulse [7].

For some molecules such as DNA, it makes more sense to perform excitation in the UV region, because the laser frequency and the electronic transition of the molecule under investigation are similar [10-11]. In the Raman process the energy that occurs because of the interaction of light with vibrational modes associated with chemical bonds within the sample is change. This shift in energy is indicative of discrete vibrational modes of polarizable molecules, and thus a qualitative measurement of biochemical composition can be obtained. Raman spectra can infer quantitative information, provided that the instrument response function is adequately corrected. For this reason below it is describe another aspect of UV radiation.Let's start from the traditional method of decontamination of liquids using UV-C pulsed light (see Figure 4 (a)). If we have a cylinder with contaminated liquid and this cylinder is irradiated from all directions with UV radiation, the total decontamination surface is $S = 2\pi R(L+R)$, where the first term indicates the lateral surface and last term represents the surface of the bases, R, represents the radius of the base, L the length of the cylinder. So, if we use a classical method of decontamination, a big volume, of infected liquid remains contaminated $V_{cl} = \pi 2\pi R(L+R)d_p$; $V_{con} = \pi R^2 L - V_{cl} \square V_{cl}$, where V_{cl} represent the efficient contamination volume, $d_p \sim \lambda$ is the penetration depth in liquid of UV radiation. Below we offer a method of decontamination using metamaterials for increasing of the decontamination volume. Sensing properties are expected to be related to nano-scale system dimensions. Let us firstly estimate the contact surface of flowing gas or liquid. In order to increase the contact surface of the contaminated liquid, below we proposed to examine the propagation of UV radiation through two types of meta-materials: type A corresponds to the packing of photonic-crystal fibers (PCF) and type B- photonic crystals (PC) (see Figues 4 (b) and (c) respectively), which both metamaterials are transparent for *UV* spectrum. If the PCF system is placed in a cylinder with contaminated liquid (see Figure 4(a, b, c)), the liquid will fill all the space between the fibers. The decontamination surface increases substantially $S_d = \pi r(r + 2rLN)$, where N is the number of fibers from PCF, r is the radius of one fiber. Last term represents the lateral surface of the fibers. Here, it is con-

sidered that the UV radiation is inserted by fibers in the cylinder, see Figues 4 (b). The penetration depth of UV radiation (evanescent field) depends on the relative refractive indexes of fibers and contaminated liquid. Let's find the connection with classical method of decontamination. For this we need to express the decontamination area through the number of fibers. The estimations show that small radius of fiber r is proportional to $r \sim R/\sqrt{N}$. It is easy to obtain the following expression for decontamination area of N cylindrical fibers $S_d \sim 2\pi RL\sqrt{N}$. Here, we observe that the decontamination surface is proportional to the square root from the number of fibers.

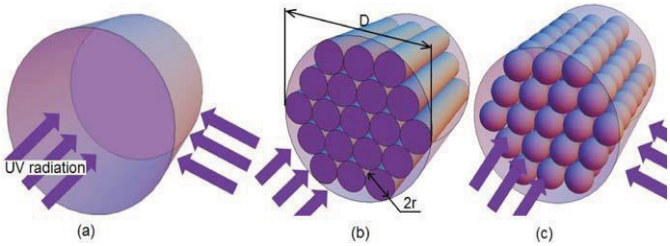


Figure 4. Methods of decontamination: (a) traditional decontamination; (b) decontamination using PCF in the hexagonal packed bundle; (c) metamaterial like photon crystal.

The decontamination volume of liquid in this case is proportional to the expression $V_d \sim 2\pi RLd\sqrt{N}$. It is not difficult to observe, that the increasing of decontamination volume is proportional to $\sqrt{N}$ where $(V_d / V_{cl} \sim \sqrt{N})$.

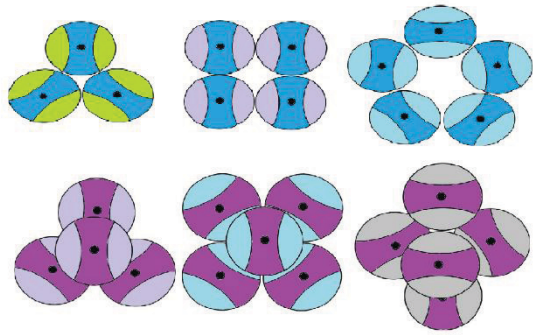
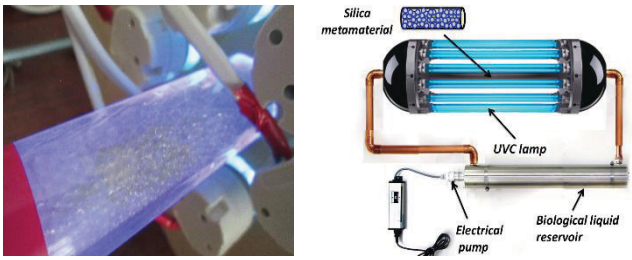


Figure 5. The possibilities of the arrangement of quantum cavities.

But it is not clear what happens with other free volume between the fiber, which is situated at larger distance in comparison with $\lambda/2$. This volume may be involved in the contamination zone, if we continue to decrease the thickness of fiber. We may estimate the free volume between the fiber and the possibility to use all this volume with the decreasing of the fiber diameter. In the standard hexagonal packed bundle we

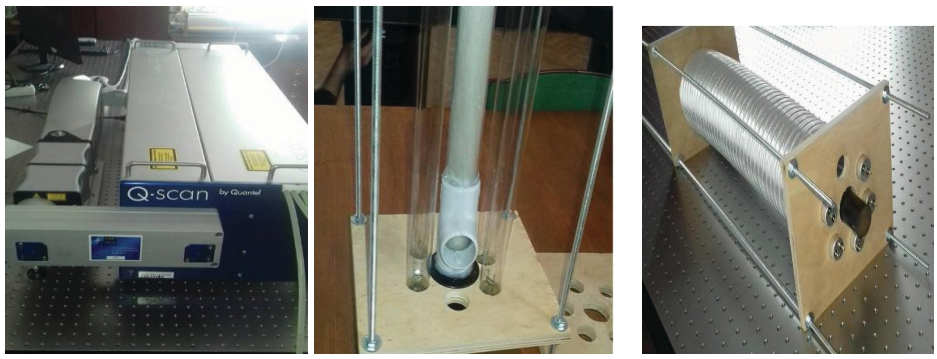
may estimate the free volume between three fibers $v_f = r^2(\sqrt{3} - \pi/2)L \approx 0.18r^2L$. In this case the free volume in the big bundle doesn't depend on the fiber diameter and is equal to $V_f = \pi R^2 L(\sqrt{3} - \pi/2)$. The unused volume may be estimated $V_a = \pi RL(0.18R - \sqrt{N}\lambda)$. When this expression achieved zero value all volume between the fiber can be used for decontamination of fluids. This corresponds to the following expression of fiber radius $r \sim R/\sqrt{N} \sim \lambda/0.18.$ The similar expression can be obtained for other type of packing of the fibers. Using the same method, we have estimated the decontamination surfaces of metamaterials (see Figure 2(Lc_1, Lc_2, Lc_3)) like PC $S_d = 4\pi r^2 N \sim \pi L^2 N^{1/3}$, where L is the edge length of the cube, r is the radius of one micro-sphere, N is the number of micro-spheres of the metamaterial. The liquid will fill all space between micro-spheres. The decontamination volume can be expressed in following form $V_d \sim dS_d = 4\pi dR^2 N^{1/3}$. Although, at first glance it appears that the decontamination volume is lower than in PCF case, this is only an illusion. Due to the fact that number of micro-spheres in metamaterial like PC is much larger than the number of fibers in PCF, the decontamination volume in the second case is much higher. The free volume between the large cube with dimension L have same proportion $V_{fr} = 0.48V$. In this case the difference between the $V_{fr} - V_d$ is proportional to $V[0.1/3/(2L)]$. When the $L < \pi N^{1/3}/0.98$, the increasing of surface becomes impossible and the classical aspects of evanescent zone is not acceptable. In this case, the volume between the balls may be regarded as a decontamination free volume. The wave is regarded as a quantum cavity for the standing wave (see Figure 5). The metamaterials, such as optical fibers or periodic photon structures open the novel possibilities to manipulate and kill viruses and bacteria in contaminated zones of liquids or organic tissue. For example, the good contact area between the implant and cells can be accomplished using such metamaterials on the surfaces [14-15]. The guided UV radiation along the implant surface maintains the best medical assistance of contact surface against possible viruses or bacteria. The UV action against bacteria and viruses depends on the depth and volume of the evanescent zone of the periodical waveguide structures. In Figures 6 and 7, is represented such a periodical structure (fibres and spherical metamaterials), introduced into a cylinder through which the contaminated fluid flows**.** Taking into consideration the traditional conception of decontamination and possible decontamination volume in the evanescent zones of fibres or periodical bubble structures (see Figure 4), we may introduce the relative decontamination coefficient $\rho = V_d/V_c$. Considering that the lateral surface of the cylinder is larger than the surfaces of its two bases, is obtained the following expression for the relative decontamination volume $\rho \sim d\sqrt{N}/d_p$**.** The similar expression can be introduced and for metamaterials like PC if we filled the cylinder with periodical bubbles of SiO_2. In this case the relative decontamination coefficient is $\rho \sim dN^{1/3}/d_p$**.** Here the classical decontamination volume is considered the penetration of the radiation into the spherical elementary volume $4\pi R^2 d_p$ with the width $\Delta R \sim d_p$.



(a) (b)

Figure 6. The UV radiation is generated by 6 UVC lamps and it is reflected in the center of decontamination region, where it is placed a cylinder, filled up by quartz microspheres. The cylinder filled up by quartz microspheres (a). Schematic representation of reactor for UV decontamination (b).

Considering that the lateral surface of the cylinder is larger than the surfaces of its two bases, we obtain the following expression for the relative decontamination volume. The combination of SiO_2 PC with PCF improved the decontamination contact surface according to our preliminary investigations. The research of the efficient action of *UV* pulses on the chemical reactions, which take place in the microorganisms is in the initial stage of our studies. Another effect which can appear in the process of decontamination is connected with the trapping of pathogen particles (viruses and bacteria) near the surface of fibers (or spheres). This effect is well known in the literature [5]. It consists in the attractive force acting on the particles with higher refractive indexes relative the refraction index of liquid index and appears due to the large gradient of EMF in the evanescent zone near the fibre Figure 4 (sphere Figure 6(a). The system of quartz fibers with periodical structures irradiated simultaneously with 5 UV-C lamp and nanosecond laser pulses effectively decontaminates the bacteria and fungi (yeast) present in translucent fluids.



(a) (b) (c)

Figure 7. The preparation of mixed decontamination equipment, which use the UVC lamps and laser pulses (a). On the bottom part of the figure is applied the canal for laser beam represented by black circle (b). The final version of decontamination equipment in which laser pulses are sent through the black part of central core (c).

The process of development of this equipment which use both method of decontamination is presented in Figure 7. The Q-scan is a high resolution nanosecond dye laser ranging from 200 nm to 4.5 μm see Figure 7(a). The last studies demonstrate that the UVC radiation becomes the effective method for inactivating bacteria, viruses, fungi and other micro-organisms. According to the literature [1-14] the special UVC radiation is an effective, environment-friendly and chemical-free method to dystrophy dangerous pathogens in any condition. On the other hand, UVC doesn't pass the atmosphere, so it normally doesn't contribute to DNA damage, but it deserves to be mentioned that UVC lamps are used to kill bacteria and bedbugs. As a consequence, a local vibration energy of the modes may be coupled by an-harmonic non-linear term. For example, two vibration defects in cell replication and lead to cell death afterwards. The increasing of popularity of fiber system interaction with fabrics structures of clothing and the diversity of the optical schemes and methods of decontamination opens the opportunities for innovative research performing in this area. The scientific studies are stimulated also by a lot of incidence of short and long-term complications in the hazard situations, which took place decontamination of infected the fabrics (for example fabric clothing) used by people. One of them is when the fabric for cloth clothing adhesion with UVC is not in a good compatibility with decontamination sources (is not transparent or scatter the radiation so that the decontamination in the volume of material becomes impossible). Taking into consideration the metamaterials popularity, like PCF, it was decided to use these optical systems in their adhesion and penetration into a volume of fabrics killing the pathogens from fabrics and rooms inventory.

CONCLUSIONS

It is propose new methods of decontamination with applications in medicine and public health. These methods contribute to an important increasing of the rate and volume of decontamination by increasing the contact zone between the light radiation and the contaminated environment (gases, liquids and solid surfaces). Regarding implants, a fine metamaterial coating on the implant surfaces not only contributes to the decontamination of the implant-tissue contact, but can also be beneficial for improving both of mechanical contact between the optic network of the metamaterial - patient's organic tissue and the processes taking place in immediate proximity to the irradiation area. A special attention will be paid to the propagation of short light pulses through such metamaterials. They will provide a selective interaction with the pathogen biomolecules having a negligible destructive action on human tissue components. The paper contains both an application and a fundamental aspect. Many of the effects of decontamination and capture of viruses and bacteria along metamaterial surfaces are seen, for example, in the transport of nutrients to the surface of tubules. So the development of metamaterial contact techniques with organic tissue opens up new possibilities for the prevention, monitoring and treatment of pathogenic diseases in different environments, including implantology. Here it can refer to different types

of implants, such as implants for the heart, wrists implants, dental implants. Another field of application of the proposed decontamination methods directly addresses the issues of selective decontamination of the blood components. An important aspect of the fundamental part of the paper it is present the development of the vibrational model of microorganism inactivation for a deeper understanding of the non-thermal selective action mechanisms on microorganisms taking into account both the duration, frequency and intensity of radiation pulses, as well as the basic characteristics of pathogens (dimensions, form, including capsid viruses, encapsulated or non-encapsulated viruses, internal symmetry of protein structures, types of bonds in biomolecules, single / double stranded nucleic acids).

REFERENCES

1. BLOEMBERGEN, N. & SHEN, Y. R. *Quantum-theoretical comparison of nonlinear susceptibilities in parametric media, lasers and Raman lasers*. Phys. Rev. 1963 133: A37-49.
2. BEGLEY, R. F. et al. *Coherent anti-Stokes Raman spectroscopy*, Appl. Phys. Lett. 1974, 25, 387-390.
3. QIANG, Tu. et al. *Diagnostic applications of Raman spectroscopy*, Nanomedicine 8, 2012, 545–558.
4. MANNIGE, R. V. et al. *Periodic Table of Virus Capsids: Implications for Natural Selection and Design. Periodic Table of Virus Capsids: Implications for Natural Selection and Design.* 2010, PLoS ONE 5(3): e9423.
5. ALMAR, F. P. et al. *Raman and SERS microscopy for molecular imaging of live cells, Nature protocols*, 2013, VOL.8 NO.4, p. 677-692.
6. KATHERINE, J. I. et al. *Raman spectroscopy and regenerative medicine: a review*, npj Regenerative Medicine, volume 2, number 12, 2017, pp. 13.
7. TURCAN, M. et al. *Cooperative generation of entanglement states by Raman conversion of photons in nano-Fibers*, Rom. Rep. in Phys., Volume 67, No. 4, 2015, p. 1334–1340.
8. YONZON, C. R. et al. *A glucose biosensor based on surface-enhanced Raman scattering: improved partition layer, temporal stability, reversibility, and resistance to serum protein interference*. Anal. Chem. 76, 2004, p. 78–85.
9. POTCOAVA, M.C. et al. *Raman and coherent anti-Stokes Raman scattering microscopy studies of changes in lipid content and composition in hormone-treated breast and prostate cancer cells*, Journal of Biomedical Optics 19(11), 2014, p.111605-11.
10. HOLLY, J. B. et al. *Using Raman spectroscopy to characterize biological materials*, Nature protocols Volume 11, No. 4, 2016, p. 664-687.
11. VO-DINH, T. *Biomedical Photonics Handbook: Biomedical Diagnostics* Vol. 2 (CRC press, 2014).

12. TSEN, S. W. D. et al. *Prospects for a novel ultrashort pulsed laser technology for pathogen inactivation,* Journal of Biomedical Science 19, 62, 2012.
13. LOUDON, R. *The Quantum Theory of Light*, Oxford University Press, 2000, pp. 448.
14. BAZGAN, S. . et al. *Propagation of UV radiation through meta-material and its application in bio decontamination*, 2015, Rom. Rep. Phys. 67 (4), pp. 1602–1607.
15. ENAKI, N. *Cooperative properties of multiple quantum scattering: I quantum nutation..* Phys Scripta, 2024, 99(4), 045102. Doi: 10.1088/1402-4896/ad29cb (IF: 2,9).
16. ENAKI, N. et al. *Metamaterials for Antimicrobial Biofilm Applications: Photonic Crystals of Microspheres and Optical Fibers for Decontamination of Liquids and Gases*, ch. 13. 27 p., Handbook of Antimicrobial Coatings, 1st Edition, Authors: Atul Tiwari, eBook ISBN: 9780128119839, Elsevier, 2018, pp. 596.
17. NAHAR, Q. et al. *Waveguide evanescent field scattering microscopy: bacterial biofilms and their sterilization response via UV irradiation*, J. Biophotonics 7(7), 2014, 542–551.
18. DAI, T. et al. *Ultraviolet C irradiation: an alternative antimicrobial approach to localized infections?* 2012 Expert Rev Anti Infect Ther 10, 185–195.
19. MUNTEANU, I. et al. *Ultraviolet C intensity dependence of de-contamination efficiency for pathogens as function of repacked metamaterials with screw channels*. Eur Biophys J. 2024, 53(3), 133—145. (IF: 2,0).

Acknowledgements
This work was supported by the project: ANCD 20.80009.5007.01.